Synthesis and Formation Mechanism of Manganese Dioxide Nanowires/Nanorods

Xun Wang and Yadong Li*[a]

Abstract: α-, β-, γ-, and δ-MnO_2 single-crystal nanowires/nanorods with different aspect ratios have been successfully prepared by a common hydrothermal method based on the redox reactions of MnO_4^- and/or Mn^{2+}. The influences of oxidant, temperature, and inorganic cation (NH_4^+ and K^+) template concentrations on the morphology and crystallographic forms of the final products are discussed in this paper. It is interesting to find that all the MnO_2 one-dimensional nanostructures have a similar formation process: δ-MnO_2, which has a layer structure, serves as an important intermediate to other forms of MnO_2, and is believed to be responsible for the initial formation of MnO_2 one-dimensional nanostructures. A rolling mechanism has been proposed based on the results of the series of TEM images and XRD patterns of the intermediate.

Keywords: manganese · nanostructures · rolling mechanism · template synthesis

Introduction

For many years, manganese dioxides and derivative compounds have attracted special attention, because of their outstanding structural flexibility combined with novel chemical and physical properties, which are of interest for the following applications, for example, molecular sieves, catalysts, and Li/MnO_2 batteries.[1–15] Different structural forms of MnO_2 exist in nature, such as the α-, β-, γ-, and δ-types.[2] The crystallographic forms are generally believed to be responsible for their properties,[2, 3] and the controlled synthesis of MnO_2 has always been the focus of material scientists.[1, 3, 4, 6, 8, 15–18] Meanwhile, with the development of one-dimensional nanostructures, dimensionality and size of the materials have also been regarded as critical factors that may bring some novel and unexpected properties: for example, isotropic or anisotropic behavior and region-dependent surface reactivity, etc. So the synthesis of manganese dioxides with well-controlled dimensionality, size, and crystal structure should be of great significance.

On the basis of the redox reactions of MnO_4^- and/or Mn^{2+}, several methods have been developed to prepare MnO_2 with different crystallographic forms, such as thermal,[8] reflux[9, 10, 11] hydrothermal,[6, 11, 15] and sol-gel,[17, 18] etc. The influences of pH, countercations, temperature, concentrations, and anions on the crystallinity and crystal forms of the final products have been extensively studied. Particularly, the effects of inorganic cation templates[19] on the formation of different tunnel structures should be critical, as the tunnels of different MnO_2 crystal forms have different sizes and need different amounts of cations to stabilize. In most of the previously reported synthetic routes, these properties have been controlled through the adjustment of the pH, with the H_3O^+ and/or H_2O as possible stabilizing and/or molecular ions,[9] for example, α-MnO_2 tends to be favored in aqueous concentrated acid, [9, 10, 11] whereas δ-MnO_2 forms preferentially in aqueous concentrated base.[16] In this paper, we will present a controllable, hydrothermal synthetic method for the preparation α-, β-, γ-, and δ-MnO_2 with the concentration of inorganic cations (NH_4^+ and K^+) as the main influencing factors and pH left just as it is. It is worth noting that all the products examined have nanowires/nanorods morphologies, which may bring some novel properties for their reduced dimensionality.

Although α- and Tokorokite-type MnO_2 have been found to have fiber or needle morphologies,[6, 11, 15] few studies have been focused on the synthesis of MnO_2 nanowires/nanorods with different crystal structures,[10, 20, 21, 22] especially about their formation process. In fact, despite the several successful techniques in the synthesis of one-dimensional nanostructures, such as thermal evaporation,[23] nanotube or mesoporous materials confinement,[24, 25] solution-based synthesis,[26, 27, 28, 29] microemulsion,[30] vapour-liquid-solid (VLS) growth,[31, 32] etc., there is still a lack of a general understanding about the anisotropic growth of one-dimensional

[a] Prof. Y. Li, X. Wang
Department of Chemistry
Key Laboratory Atomic & Molecular Nanosciences
Ministry of Education
Tsinghua University, Beijing, 100084 P. R.(China)
Fax: (+86) 10-62788765
E-mail: ydli@tsinghua.edu.cn

Supporting information for this article is available on the WWW under http://www.chemeurj.org or from the author.

0947-6539/03/0901-0300 $ 20.00+.50/0

nanostructures. Very recently, in our synthesis of Bi,[33] WS_2,[34] titanate, and [35] VO_X[36] nanotubes and W nanowires,[37] we have found that one-dimensional nanostructures can be obtained from the rolling of a natural or artificial lamellar structure. Under certain conditions, a layer structure may begin to curl (the interaction between the neighboring layers could be reduced from the edges of the layer, while keeping the interactions of the in-layer atoms or molecules), and the thus-obtained tubular structure may serve as the original driving force for the growth of one-dimensional nanostructures.[34] A clear understanding about the bending of the graphite under high temperature or electron beam irradiation has been elucidated;[38, 39] this further strengthens the possibility of the rolling process of a lamellar structure. Among the several crystallographic forms of MnO_2, δ-MnO_2 alone has a layer structure,[2] which is indispensable in the rolling mechanism. So our studies have been focused on the role that δ-MnO_2 plays in the formation of the other structural MnO_2 one-dimensional nanostructures. According to our experiment results, δ-MnO_2 serves as an important intermediate to other forms, and is responsible for the formation of MnO_2 one-dimensional nanostructures.

Results and Discussion

Phase-controlled synthesis of α, β-, and γ-MnO_2 nanowires/nanorods by a liquid-phase oxidation method: With Mn^{2+} as the main Mn source, α-, β-, and γ-MnO_2 nanowires/nanorods could be obtained by a liquid-phase oxidation method (Table 1).

$(NH_4)_2S_2O_8$ was used as the oxidizing reagent for $MnSO_4$, and the whole reaction is given in Equation (1):

$$MnSO_4 + (NH_4)_2S_2O_8 + 2H_2O \rightarrow MnO_2 + (NH_4)_2SO_4 + 2H_2SO_4 \quad (1)$$

Under hydrothermal conditions, α- and β-MnO_2 were obtained by varying the concentration of NH_4^+ and SO_4^{2-}, which coexist with the corresponding ions Mn^{2+} and $S_2O_8^{2-}$ in the reaction system. The final products of direct reaction of $(NH_4)_2S_2O_8$ and $MnSO_4$ is β-MnO_2 (Figure 1B, JCPDS 24-0735); however, if the direct reaction occurs at 90 °C, 1 atm, γ-MnO_2 (Figure 1C) is obtained. The phase changes to α-MnO_2 (Figure 1A, JCPDS 44-0141) when certain amount of $(NH_4)_2SO_4$ (e.g., 0.02 mol) is introduced to the reaction system.

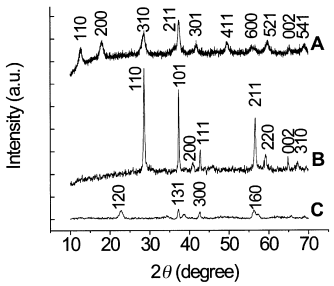

Figure 1. A) XRD pattern of α-MnO_2 (sample 3); B) XRD pattern of β-MnO_2 (sample 1); C) XRD pattern of γ-MnO_2 (sample 2).

All the α-MnO_2 samples have a ribbonlike nanowires morphology with diameters of 5–20 nm and lengths ranging between 5 and 10 μm. As is shown in Figure 2A, most of the α-MnO_2 nanowires have a smooth texture, and some of them are slightly bent. The β-MnO_2 phase was observed to exist as nanorods with diameters 40–100 nm and lengths ranging between 2.5–4.0 μm (Figure 2B). The aspect ratios of β-MnO_2 change with the concentration of $(NH_4)_2SO_4$, as can be seen in Figure 2C. Compared with α- and β-type, γ-MnO_2 has a smaller aspect ratio of 5–10 (Figure 2D). High-resolution TEM images of α- and β-MnO_2 as well as electron diffraction patterns from a single rod of the corresponding samples are shown in Figures 2E and F, respectively.

Although pH is generally believed to have great impact on the crystal forms of the final products,[9, 10, 11, 16] in our system, the pH is relatively stable (kept at about 2.5), and does not change much with the addition of $(NH_4)_2SO_4$ to the system; so the key to different crystal forms does not appear to be the pH.

It is apparent that pressure and ion concentration (NH_4^+ and SO_4^{2-}) have played an important role in determining the crystal structure and morphology of the final products. α-, β-, and γ-MnO_2 are all constructed from chains of $\{MnO_6\}$ octahedra, which are linked in different ways so that they have 2×2, 1×1, and 1×2 tunnels in their structures, respectively. Under the hydrothermal conditions, it seems that the symmetrical structures of 1×1 and 2×2 tunnels are more stable and can be easily obtained. As far as the less symmetrical structure of 1×2 tunnels is concerned, a lower pressure is necessary, as has been proved by the formation of γ-MnO_2 at 1 atm. This may also be the reason why we cannot get γ-MnO_2 by simply changing the concentration of NH_4^+ under hydrothermal conditions, in contrast to the preparation of α-MnO_2. The concentration of $(NH_4)_2SO_4$ can be regarded as the key

Table 1. MnO_2 nanowires/nanorods obtained under different reaction conditions.

Sample	Experimental conditions			Phase	Morphology		
	oxidant	T [°C]	$(NH_4)_2SO_4$ [mol]		diameter [nm]	length [μm]	% nanowires
1	$(NH_4)_2S_2O_8$	140	0	β	40–100	2.5–4.0	>95
2	$(NH_4)_2S_2O_8$	90	0	γ	20–40	0.1–0.2	>90
3	$(NH_4)_2S_2O_8$	140	0.02	α	5–20	5–10	>95
4	$(NH_4)_2S_2O_8$	140	0.007	β	20–30	5–10	>95
5	$(NH_4)_2S_2O_8$ (0.0008 mol)	140	0.0022	α	200–400	1–3	>85
6	NaClO	180	0	β	30–40	1–2	>90
7	NaClO	180	2 mL HCl	β	60–80	0.5–1	>80
8	NaClO	180	0.02 (NH_4Cl)	β	20≈40	4–8	>90

  0947-6539/03/0901-0301 $ 20.00+.50/0

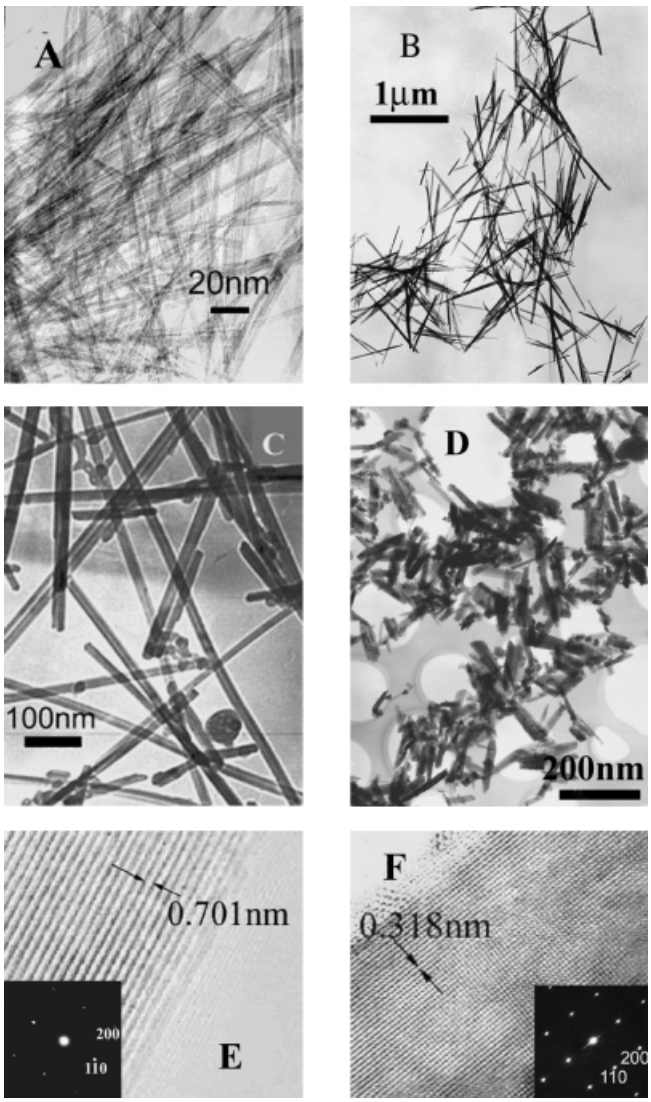

Figure 2. A) TEM image of the α-MnO_2 ribbonlike nanowires (sample 3); B) TEM image of β-MnO_2 nanorods (sample 1); C) TEM image of β-MnO_2 nanorods (sample 4); D) TEM images of γ-MnO_2 nanorods (sample 2); E) HRTEM image of α-MnO_2 (sample 3), spacing $d = 0.701$ nm, and electron diffraction pattern; F) HRTEM image of β-MnO_2 (sample 1), spacing $d = 0.318$ nm, and electron diffraction pattern.

factor in the synthesis of α- and β-MnO_2 nanowires. Certain amounts of NH_4^+ are needed to stabilize the 2×2 tunnel structure in the synthesis of α-MnO_2. To control the aspect ratios of the final products, we employed a strategy of varying the concentration of SO_4^{2-}. Based on the experiment results, a higher ion concentration is beneficial for the anisotropic growth of MnO_2, and results in a much narrower rod. Since no additional ions are added in our synthesis, higher purity will be expected.

Temperature and reactant molecular concentration can also influence the morphology of the products. It is generally believed that temperature can affect crystal growth in several ways, all of them resulting in smaller crystal size at lower temperature. From our experiments, a higher temperature is preferable for the anisotropic growth of crystal, and results in a product with higher aspect ratios. At a lower concentration, shorter nanorods will be obtained (Table 1, sample 5). In our adopted temperature range (100–180 °C), the phase does not change with the temperature, and the crystallinity decreases with the decrease in temperature.

The influence of the anion on the crystal forms of the products have been studied by Kijima et al.,[9] and they found that α-MnO_2 tends to form in concentrated H_2SO_4 instead of HCl or HNO_3. To investigate the effects of different anions, NaClO was used to oxidize Mn^{2+} with NH_4Cl as a possible template; however, this resulted in the formation of β-MnO_2 only. By increasing the concentration of NH_4Cl, a product with the same phase and less crystallinity is obtained, and an excess amount of NH_4Cl leads to the formation of a low-valence-state manganese oxide mixture. We have tried to control morphology of the final products by adding NH_4Cl or HCl (concentrated, 2 mL) to the system; the aspect ratios of the products also changed (see Table 1 and the Supporting Information).

Phase-controlled synthesis of α, β-, and δ-MnO_2 nanorods by a comproportionation method: For this method $KMnO_4$ was used as the oxidizing reagent for $MnSO_4$, and the whole reaction is given in Equation (2):

$$2\,KMnO_4 + 3\,MnSO_4 + 2\,H_2O \rightarrow 5\,MnO_2 + K_2SO_4 + 2\,H_2SO_4 \quad (2)$$

On the other hand, $KMnO_4$ decomposes in solution[40] and so we get Equation (3):

$$KMnO_4 + [(1-x+2y)/2]\,H_2O \rightarrow K_xMnO_2 \cdot y\,H_2O + (1-x)\,KOH + [(3+x)/4]\,O_2 \quad (3)$$

Suib et al. have prepared α-MnO_2 by a similar hydrothermal method with the same reaction, in which pH plays an important role in influencing the crystallographic form of the final products; the β-type was obtained when the temperature was kept above 120 °C.[11] In our experiment, we found that just by varying the molar ratio of $KMnO_4$ and $MnSO_4$, MnO_2 nanorods with different crystallographic forms could be obtained in a wide temperature range without adjusting the pH of the system, and even at a temperature as high as 180 °C, α-MnO_2 could also be obtained.

In our experiment, δ-MnO_2 nanorods (Figure 3C, indexed to JCPDS 80-1098 and Figure 4D) have been obtained when

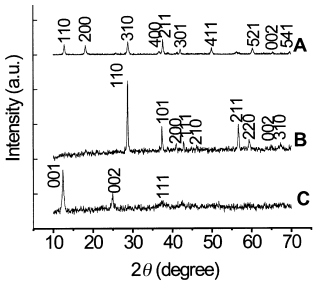

Figure 3. A) XRD pattern of the α-MnO_2 nanorods obtained from the $KMnO_4/MnSO_4$ reaction system (2.5:1, 160 °C). B) XRD pattern of the β-MnO_2 nanorods obtained from the $KMnO_4/MnSO_4$ reaction system (2:3, 160 °C). C) XRD pattern of the δ-MnO_2 nanorods obtained from the $KMnO_4/MnSO_4$ reaction system (6:1, 160 °C).

0947-6539/03/0901-0302 $ 20.00+.50/0 *Chem. Eur. J.* **2003**, *9*, No. 1

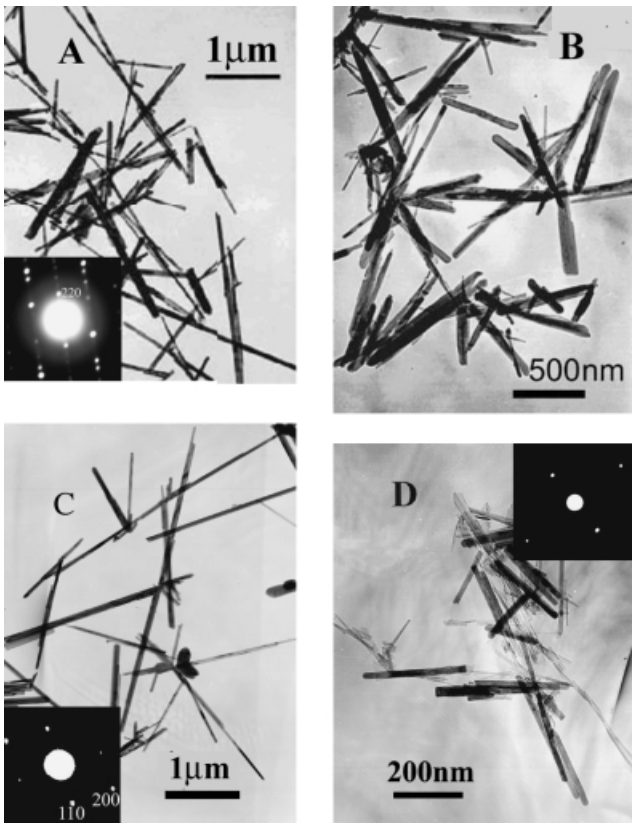

Figure 4. A) TEM image of α-MnO_2 nanorods obtained from the $KMnO_4$/$MnSO_4$ (2.5:1, 180 °C) reaction system; B) TEM image of β-MnO_2 nanorods obtained from the $KMnO_4$/$MnSO_4$ (2:3, 160 °C) reaction system; C) TEM image of β-MnO_2 nanorods with larger aspect ratios obtained from the $KMnO_4$/$MnSO_4$ (1:1, 160 °C) reaction system; D) TEM image of δ-MnO_2 nanorods with larger aspect ratios obtained from the $KMnO_4$/$MnSO_4$ (6:1, 160 °C) reaction system.

pure $KMnO_4$ or a high molar ratio (around 6:1) of a $KMnO_4$/$MnSO_4$ mixture is hydrothermally treated at 160 °C. When the molar ratio of $KMnO_4$/$MnSO_4$ is controlled at about 2.5:1, the products prove to be α-MnO_2 (Figure 3A) naorods with diameters 20–80 nm and lengths ranging between 2 and 6 μm (Figure 4A). When the molar ratio is adjusted to about 2:3, the reaction results in β-MnO_2 (Figure 3B) nanorods with diameters 40–100 nm and lengths 0.5–1.0 μm (Figure 4B). The single-crystal nature of the α-, β-, and δ-MnO_2 nanorods are revealed by the electron diffraction patterns, which were taken from a single rod of each of the corresponding samples. The percentage of nanorods formed could be readily kept above 95 % in typical α- and β-MnO_2 samples, and a value of about 70 % was obtained in δ-MnO_2 samples.

It might be believed that only reaction (2) occurs at a molAr ratio of 2:3, while a combination of reactions (2) and (3) will occur simultaneously at molar ratios of 2.5:1 and 6:1.

The concentration of K^+ ions may be the key to phase-controlled synthesis, since no additional OH^- or H^+ are added to the system and the pH does not change much when molar ratio is changed. The α-, β-, and δ-MnO_2 phases have 2×2, 1×1 tunnels, and layer structures, respectively. The K^+ ion can serve as a template in the formation of these tunnel or layer structures;[19] however, different amounts of K^+ are needed for the formation of different structures. Layer structures may need more cations or H_2O molecules to be stable. So δ-MnO_2 is produced at a higher K^+ concentration, while α- and β-MnO_2 are obtained at comparatively lower K^+ concentrations with molar ratios adjusted to 2.5:1 and 2:3, respectively.

The aspect ratios of the pure phase α-MnO_2 nanorods change if the molar ratio of $KMnO_4$/$MnSO_4$ is varied between 3:1 and 1.75:1, while β-MnO_2 single-crystal nanorods with tunable morphologies can be obtained in the range of 1:1 and 2:3 (Figure 4C).

Temperature also has an influence on the morphology of different MnO_2 nanorods to some extent; however, this is a less influential factor compared with the mole ratio.

The formation mechanism of MnO_2 one-dimensional nanostructure under hydrothermal conditions: From the above experimental results, although the Mn sources are different, the MnO_2 one-dimensional nanostructures have been obtained in similar ways. Considering the similarity of their structures and the comparability of the synthetic routes, do they have a common growth process to one-dimensional nanostructures? And what is the original driving force for the initial formation of rodlike nanostructures in solution? Xiao et al. have proposed that the hollandite-type MnO_2 random-weave nanofibrous structure develops from an initial nanoparticle agglomerated mass under the reflux conditions.[10] However, based on our experiment results, we prefer to believe that a rolling mechanism is responsible for the formation of MnO_2 nanowires/nanorods.

To investigate the formation process of MnO_2 one-dimensional nanostructures under hydrothermal conditions, we varied the reaction time of the synthesis: A) 20 min, B) 30 min, C) 45 min and D) 1 h. Although we know that the reaction does not stop immediately after the autoclave is removed from the heater owing to heat transfer reasons, we do believe that the precipitates we have obtained represent certain stages in the formation process.

The corresponding samples have been examined by XRD and TEM. As is shown in Figure 5B the XRD patterns of α-MnO_2 in a $(NH_4)_2S_2O_8$/$MnSO_4$ reaction system, taken after 30 min hydrothermal treatment, can be readily indexed to that of δ-MnO_2. All the samples dispersed on the TEM grids show lamellar structure morphologies (Figure 6A). Most of them have shown the tendency to curl, and some of them have grown into a tubular structure (Figure 6B and C). When the

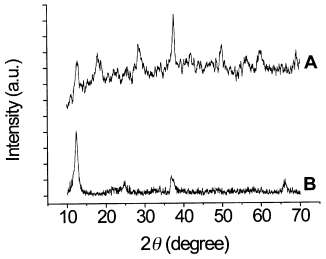

Figure 5. A) XRD pattern of the α-MnO_2 intermediate (Table 1, sample 3) after hydrothermal treatment for 2 h; B) XRD pattern of the α-MnO_2 intermediate (Table 1, sample 3) after hydrothermal treatment for 30 min.

  0947-6539/03/0901-0303 $ 20.00+.50/0

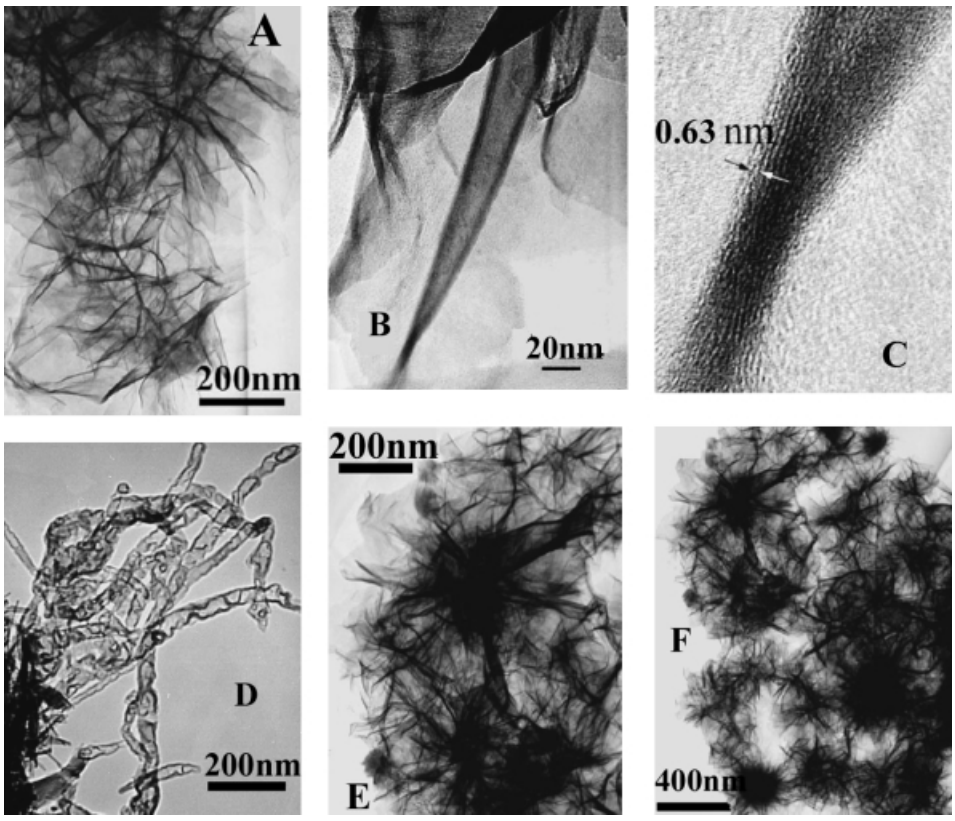

Figure 6. A) TEM image of the α-MnO_2 intermediate (Table 1, sample 3) after hydrothermal treatment for 30 min; B) HRTEM image of the curling intermediate (from Figure 7A) after hydrothermal treatment for 30 min; C) HRTEM image of the corresponding part in Figure 7B; D) TEM image of the α-MnO_2 tubular intermediate (Table 1, sample 3) after hydrothermal treatment for 45 min; E) TEM image of the α-MnO_2 intermediate ($KMnO_4$/$MnSO_4$, 2:1, 160 °C) after hydrothermal treatment for 1 h; F) TEM images of the β-MnO_2 intermediate ($KMnO_4$/$MnSO_4$, 2:3, 160 °C) after hydrothermal treatment for 30 min.

reaction time is prolonged to 45 min, tubelike structures are observed (Figure 6D). However, after a further prolonged reaction time (1.5 h), the curling and tubelike structures disappear, and only shorter nanowires are obtained; the XRD patterns of the samples show a great similarity to that of α-MnO_2 with a less crystallinity (Figure 5A).

According to the XRD patterns of the intermediate (30 min and 1.5 h), a $\delta \rightarrow \alpha$ phase transformation must have taken place in the formation process of α-MnO_2; this is reasonable since δ-MnO_2 has been used as a precursor for other types of MnO_2 materials prepared by thermal decomposition or hydrothermal treatment.[6, 15] Among the several crystal forms of MnO_2, δ-MnO_2 alone has a layer structure, which has also been proved by the TEM images of the intermediate (Supporting Information). The curling and tubular structure in the intermediate, together with the XRD patterns, may serve as the most powerful proof that the rolling mechanism is responsible for the initial formation of α-MnO_2 nanowires.

Similar XRD patterns of δ-MnO_2 have also been obtained from the intermediate (after 1 h) of α-MnO_2 in a $KMnO_4$/$MnSO_4$ reaction system (Figure 7A) or the intermediate of δ-MnO_2 ($KMnO_4$ hydrothermal for 2 h; Figure 7D). TEM images of the samples show lamellar and curling structures (Figure 6E). All the information seems to indicate that although α-MnO_2 has been got from different synthetic methods, they have undergone a similar growth process.

The growth process of β-MnO_2 nanorods ($(NH_4)_2S_2O_8$/$MnSO_4$ and $KMnO_4$/$MnSO_4$ reaction systems) has also been investigated in a similar way. A similar morphology-developing process (from lamellar to nanorods) has also been observed. The XRD patterns of the intermediates (after 1 h) can be indexed to γ- and α-MnO_2 (Figures 7C and B), respectively; this indicates a different phase-transformation process. within the limitation of our experimental conditions, the XRD patterns of δ-MnO_2 as intermediates have not been obtained. However, we do not think that it means δ-MnO_2 does not exist in the formation process of β-MnO_2. As far as the concentration of stabilizing cations is concerned, the β-MnO_2 formation system is the lowest. So it would be reasonable to imagine that the collapse of the layer structure of MnO_2 occurs very quickly, and that the δ-MnO_2 stage is hard to be separated from the following stages. Actually, if we take samples from the $(NH_4)_2S_2O_8$/$MnSO_4$ system after hydrothermal treatment for 20 min or from the $KMnO_4$/$MnSO_4$ system after hydrothermal treatment for 30 min, all the TEM images show layer structures (Figure 6F and Supporting Information). Similar structure also exists in the NaClO/$MnSO_4$ system (Supporting Information). So the phase transformation of β-MnO_2 must also have a corresponding stage of δ-MnO_2.

Based on the above experimental results, we suggest that under hydrothermal conditions all the MnO_2 one-dimensional nanostructures have a common developing process, which is

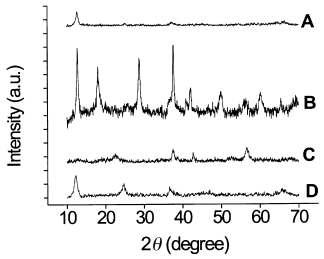

Figure 7. A) XRD pattern of the α-MnO_2 intermediate ($KMnO_4$/$MnSO_4$, 2:1, 160 °C) after hydrothermal treatment for 1 h; B) XRD pattern of the β-MnO_2 intermediate ($KMnO_4$/$MnSO_4$, 1:1, 160 °C) after hydrothermal treatment for 1 h; C) XRD pattern of the β-MnO_2 intermediate (Table 1, sample 1) after hydrothermal treatment for 1 h; D) XRD pattern of the δ-MnO_2 intermediate (pure $KMnO_4$, 180 °C) after hydrothermal treatment for 1 h.

0947-6539/03/0901-0304 $ 20.00+.50/0 *Chem. Eur. J.* **2003**, *9*, No. 1

characteristic of a rolling mechanism and phase transformation.

A possible mechanism may be defined as follows:

1) Under hydrothermal conditions the MnO_x units will appear first in the solution, and then through a condensation reaction they will form sheets of δ-MnO_2.
2) The layer structure of δ-MnO_2 tends to curl with an elevated temperature and pressure; this is the decisive step for the formation of MnO_2 one-dimensional nanostructures. Some tubular structure may appear in the system.
3) The lamellar structure of MnO_2 is in a metastable state. If there are not enough cations, the layer structure will collapse. Due to the difference in the concentration of existing cations, the collapse will take place in several ways: δ-MnO_2 will keep its structure as enough K^+ have been provided; when a moderate amount of K^+ or NH_4^+ exist, the layer structure will directly collapse into 2×2 tunnel structure of α-MnO_2; in the case of β-MnO_2, it seems that the layer structures will collapse into 2×2 ($KMnO_4$/$MnSO_4$ reaction system) or 1×2 ($(NH_4)_2S_2O_8$/$MnSO_4$ reaction system) tunnel structure at first, then into the 1×1 structure of β-MnO_2.
4) Along with the phase transformation, the tubular and curling lamellar structures will grow into nanowires.
5) During the following hydrothermal process, the shorter nanowires may redissolve into the solution phase, and the longer ones grow into much longer ones.
6) The aspect ratios of the final products are determined by the ion concentration existing in the reaction system and the anisotropic nature of the corresponding crystal structures.

Although other unknown factors may exist that influence the growth of MnO_2 one-dimensional nanostructures, such as the influence of anions, and so forth, the above mechanism is in good agreement with our experiment results.

A similar process for the formation of rods through the folding of lamella in a surfactant mesophase has been reported by Yada et al.; they found that the folding of aluminum-based flexible layers produced various precursors, which then grew into versatile morphologies including the rodlike shape.[41] Other cases have also been encountered in our synthesis of Cu_2O and CdS nanowires/nanorods.[42] All these make us believe that rolling mechanism may be a general one in solution-based template-free growth of one-dimensional nanostructures.

Conclusion

In this paper, we have developed a facile hydrothermal method for the preparation of MnO_2 nanowries/nanorods with different crystal forms by simply altering the inorganic templates concentrations. This low-temperature synthetic route, involving no catalysts or templates and requiring no precise equipment, can be easily adjusted to prepare MnO_2 one-dimensional nanostructures on a large scale. Although the Mn sources are different, MnO_2 one-dimensional nanostructures have undergone a similar formation process, which is characteristic of a rolling mechanism and phase transformation. The suggested growth mechanism is in good agreement with our experimental results and may be a general one for the growth of one-dimensional nanostructures of other compounds.

Experimental Section

Chemicals: All the chemicals were of analytical grade and used as received without further purification. Deionized water was used throughout. Manganese sulfate ($MnSO_4\cdot H_2O$), ammonium persulfate ($(NH_4)_2S_2O_8$), ammonium sulfate ($(NH_4)_2SO_4$), potassium hypermanganate ($KMnO_4$), and sodium hypochlorite (NaClO, active Cl atom $>5.2\,\%$) were all supplied by Beijing Chemical Reagent Company.

Method A: $(NH_4)_2S_2O_8$ was as the oxidizing reagent for $MnSO_4$ this method.[21] For a typical synthesis, $MnSO_4\cdot H_2O$ (0.008 mol) and an equal amount of ammonium persulfate ($(NH_4)_2S_2O_8$) were put into distilled water at room temperature to form a homogeneous solution, which was then transferred into a 40 mL Teflon-lined stainless steel autoclave, sealed and maintained at 140 °C for 12 h. After the reaction was completed, the resulting solid product was filtered, washed with distilled water to remove ions possibly remnant in the final products, and finally dried in air. The amount of $(NH_4)_2SO_4$, temperature, aging time, and pressure were altered on the basis of this synthesis.

Method B: On the basis of Method A, $KMnO_4$ was used as the oxidizing reagents for $MnSO_4$.[22] The molar ratio of $KMnO_4$ and $MnSO_4\cdot H_2O$ was varied in the phase-controlled synthesis of α-, β-, and δ-MnO_2 nanorods with the molar number of Mn atoms kept about 0.0044 mol. Temperature was kept about 160 °C for a typical synthesis, and varied in a range of 120–180 °C. Details are available in text.

Powder X-ray diffraction (XRD): The phase purity of the products were examined by XRD by using a Brucker D8-advance X-ray diffractometer with $Cu_{K\alpha}$ radiation ($\lambda=1.5418$ Å), the operation voltage and current keeping at 40 kV and 40 mA, respectively. The 2θ range 10–70° was used in steps of 0.02° with a count time of 2 s.

Transmission electron microscopy (TEM): The size and morphology of the products were observed by using a Hitachi Model H-800 transmission electron microscope, with a tungsten filament at an accelerating voltage of 200 kV. Samples were prepared by placing a drop of dilute alcohol dispersion of nanocrystals on the surface of a copper grid. Electron diffraction and energy dispersive X-ray analysis were also performed to study the single-crystal nature or element components of the samples on H-800 TEM. Structural information of the nanocrystals was measured by high-resolution transmission electron microscopy (HRTEM) on a JEOL JEM-2010F transmission electron microscope operated at 200 kV. Electron diffraction was also performed on samples during HRTEM measurements.

Acknowledgement

This work was supported by NSFC (20025102, 50028201, 20151001), the Foundation for the Author of National Excellent Doctoral Dissertation of P. R. China and the state key project of fundamental research for nanomaterials and nanostructures.

[1] J. C. Hunter, *J. Solid State Chem.* **1981**, *39*, 142–147.
[2] M. M. Thackeray, *Prog. Solid State Chem.* **1997**, *25*, 1–71.
[3] A. Perner, K. Holl, D. Ilic, M. Wohlfahrt-Mehrens, *Eur. J. Inorg. Chem.* **2002**, 1108–1114.
[4] R.Chitrakar, H. Kanoh, Y. S. Kim, Y. Miyai, K. Ooi, *J. Solid State Chem.* **2001**, *160*, 69–76.
[5] A. R. Armstrong, P. G. Bruce, *Nature* **1996**, *381*, 499–500.
[6] D. C. Golden, C. C. Chen, *J.* B. Dixon, *Science* **1986**, *231*, 717–719.
[7] B. Ammundsen, J. Paulsen, *Adv. Mater.* **2001**, *13*, 943–956.
[8] Y. Muraoka, H. Chiba, T. Atou, M. Kikuchi, K. Hiraga, Y. Syono, *J. Solid State Chem.* **1999**, *144*, 136–142.

  0947-6539/03/0901-0305 $ 20.00+.50/0

[9] N. Kijima, H. Yasuda, T. Sato, Y. Yoshimura, *J. Solid State Chem.* **2001**, *159*, 94 – 102.
[10] T. D. Xiao, P. R. Strutt, M. Benaissa, H. Chen, B. H. Kear, *Nanostruct. Mater.* **1998**, *10*, 1051 – 1061.
[11] R. N. DeGuzman, Y. F. Shen, E. J. Neth, S. L. Suib, C. L. O'Young, S. Levine, J. M. Newsam, *Chem. Mater.* **1994**, *6*, 815 – 821.
[12] Z. M. Wang, S. Tezuka, H. Kanoh, *Chem. Lett.* **2000**, 560 – 561.
[13] L. A. H. Maclean, F. L. Tye, *J. Mater. Chem.* **1997**, *7*, 1029 – 1035.
[14] T. Kohler, T. Armbruster, E. Libowitzky, *J. Solid State Chem.* **1997**, *133*, 486 – 500.
[15] Y. F. Shen, R. P. Zerger, S. L. Suib, L. McCurdy, D. I. Potter, C. L. O'Young, *Science* **1993**, *5*, 260, 511 – 515.
[16] J. Luo, S. L. Suib, *J. Phys. Chem. B* **1997**, *101*, 10403 – 10413.
[17] S. Ching, D. J. Petrovay, M. L. Jorgensen, *Inorg. Chem.* **1997**, *36*, 883 – 890.
[18] S. Ching, J. L. Roark, N. G. Duan, S. L. Suib, *Chem.* Mater **1997**, *9*, 750 – 754.
[19] Y. F. Shen, S. L. Suib, C. L. O'Young, *J. Am. Chem. Soc.* **1994**, *116*, 11020 – 11029.
[20] Y. D. Li, C. W. Li, Y. T. Qian, Y. H. Liu, L. Q. Li, *Chem. J. Chin. Univ.* **1997**, *18*, 1436 – 1437.
[21] X. Wang, Y. D. Li, *J. Am. Chem. Soc.* **2002**, *124*, 2880 – 1881.
[22] X. Wang, Y. D. Li, *Chem. Commun.* **2002**, 764 – 765.
[23] Z. W. Pan, Z. R. Dai, Z. L. Wang, *Science* **2001**, *291*, 1947 – 1949.
[24] C. M. Lieber, *Solid State Commun.* **1998**, *107*, 607 – 616.
[25] Y. J. Han, J. M. Kim, G. D. Stucky, *Chem. Mater.* **2000**, *12*, 2068 – 2069.
[26] F. Kim, S. Kwan, J. Akana, P. D. Yang, *J. Am. Chem. Soc.* **2001**, *123*, 4360 – 4361.
[27] J. J. Urban, W. S. Yun, Q. Gu, H. K. Park, *J. Am. Chem. Soc.* **2002**, *124*, 1186 – 1187.
[28] B. Gates, Y. Y. Wu, Y. D. Yin, P. D. Yang, Y. N. Xia, *J. Am. Chem. Soc.* **2001**, *123*, 11500 – 11501.
[29] W. W. Yu, X. G. Peng, *Angew. Chem.* **2002**, *114*, 2474 – 2477; *Angew. Chem. Int. Ed.* **2002**, *41*, 2368 – 2371.
[30] M. Li, H. Schnablegger, S. Mann, *Nature* **1999**, *402*, 393 – 395.
[31] M. H. Huang, S. Mao, H. Feick, H. Q. Yan, Y. Y. Wu, H. Kind, E. Weber, R. Russo, P. D. Yang, *Science* **2001**, *292*, 1897 – 1899.
[32] X. F. Duan, Y. Huang, Y. Cui, J. F. Wang, C. M. Lieber, *Nature* **2001**, *409*, 66 – 69.
[33] Y. D. Li, J. W. Wang, Z. X. Deng, Y. Y. Wu, X. M. Sun, D. P. Yu, P. D. Yang, *J. Am. Chem. Soc.* **2001**, *123*, 9904 – 9905.
[34] Y. D. Li, X. L. Li, R. R. He, J. Zhu, Z. X. Deng, *J. Am. Chem. Soc.* **2002**, *124*, 1411 – 1416.
[35] X. M. Sun, Y. D. Li, unpublished results.
[36] X. Chen, X. M. Sun, Y. D. Li, *Inorg. Chem.* **2002**, *41*, 4524 – 4530.
[37] Y. D. Li, X. L. Li, Z. X. Deng, B. C. Zhou, S. S. Fan, J. W. Wang, X. M. Sun, *Angew. Chem.* **2002**, *114*, 343 – 345; *Angew. Chem. Int. Ed.* **2002**, *41*, 333 – 335.
[38] R. D. Heidenreich, W. M. Hess, L. L. Ban, *J. Appl. Crystallogr.* **1968**, *1*, 1.
[39] D. Ugarte, *Nature* **1992**, 359, 707 – 709.
[40] R. J. Chen, P. Zavalij, M. S. Whittingham, *Chem. Mater.* **1996**, *8*, 1275 – 1280.
[41] M. Yada, H. Hiyoshi, K. Ohe, M. Machida, T. Kijima, *Inorg. Chem.* **1997**, *36*, 5565 – 5569.
[42] Y. D. Li, et al., unpublished results .

Received: August 12, 2002 [F4337]

  0947-6539/03/0901-0306 $ 20.00+.50/0